



Supplement of

Impacts of marine organic emissions on low-level stratiform clouds – a large eddy simulator study

Marje Prank et al.

Correspondence to: Marje Prank (marje.prank@fmi.fi)

The copyright of individual parts of the supplement might differ from the article licence.

S1. Sensitivity of the results to model features and setup

In preparation of the simulations presented in the manuscript we performed a number of test simulations to quantify the sensitivity of the results to various model features and setup options.

S1.1 Model domain and resolution

All UCLALES-SALSA simulations presented in the manuscript were made with horizontal resolution of 60x60 m on a 10x10 km domain. **Figure S1** compares cloud field and precipitation from simulations with larger domain size (20x20 km) and higher horizontal resolution (50 m) (Panel A) with identical simulations using the current setup (Panel B). The larger setup was computationally too heavy to be feasible for the large number of simulations presented, however, the simulations with current setup (10x10 km domain and 60 m horizontal resolution) did not significantly differ from those in any of the variables discussed in the manuscript (see timeseries on Figure S2).

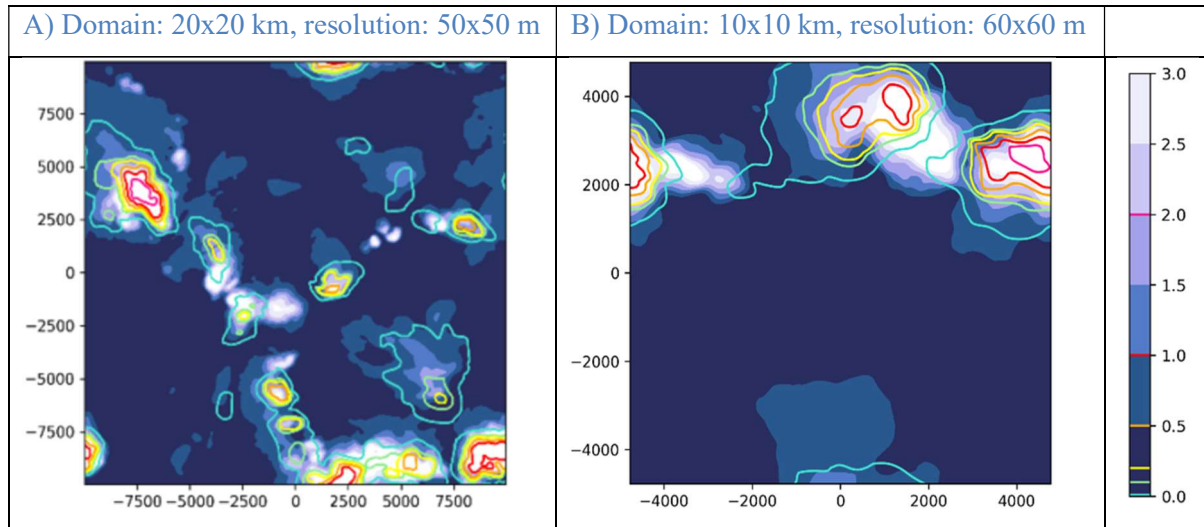


Figure S1. Cloud and precipitation pattern in comparable simulations with (A) 20 km domain, 50 m resolution and (B) 10 km domain, 60 m resolution. 10 hours after the start of the simulation. Contours – surface precipitation rate (mm/h), white shading – liquid water path (g/m^2) (scaled by a factor 0.01 to fit on same scale as precipitation).

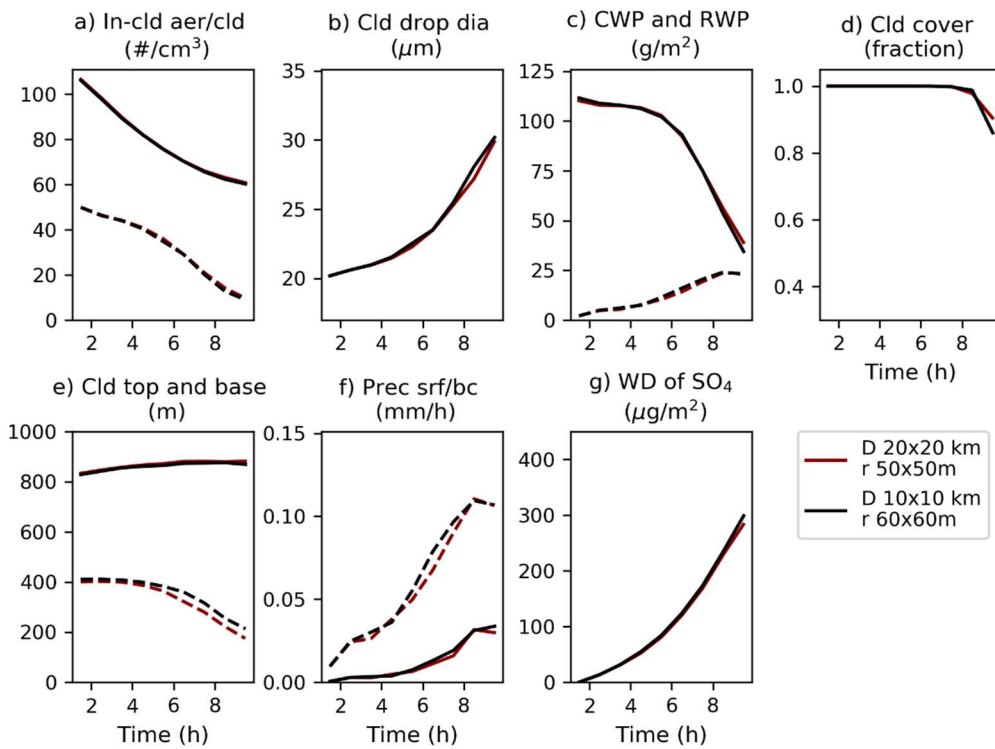


Figure S2. Timeseries of comparable simulations with 20 km domain, 50 m resolution (brown) and 10 km domain, 60 m resolution (black). Hourly averaged time series, mean over the model area. Panels: a – in-cloud cloud interstitial aerosol (solid) and cloud droplet (dashed) concentration, b – Cloud droplet size, c –Cloud liquid water path (solid) and rain water path (dashed), d – height of cloud top (solid) and base (dashed), e –precipitation rate at surface (solid) and below cloud (dashed), f – cumulative wet deposition of background aerosol (ammonium bisulfate).

We have not explicitly tested the sensitivity of UCLALES-SALSA model to the vertical resolution for this specific case, as it was optimized for the LES intercomparison study by Ackerman et al. (2009). The resolution is less than 25 meters for all in-cloud and below-cloud layers and 5 meters in the regions with largest gradients (near surface and cloud top). Stevens et al. (2005) tested the sensitivity of LES models to the resolution at cloud top for the Research flight 1 of the DYCOMS II campaign and showed no further improvement with resolutions better than 5m. Tonttila et al. (2021) show very small difference between 5 and 10 meter model vertical resolutions with UCLALES-SALSA model, although for a different case.

S1.2 Model noise

In the preliminary testing phase, we also investigated the model noise by performing two almost identical simulations that differed only by the random fluctuations in the temperature field used to initialize the turbulence. The results of this experiment are shown on Figure S3. Expectedly, the noise is largest in the precipitation flux, while other quantities do not show large discrepancies, with the exception of cloud drop size at the very end of the simulation. Any simulation results differing from each other in similar level to what is shown on Figure S3 have been considered identical when analysing the results.

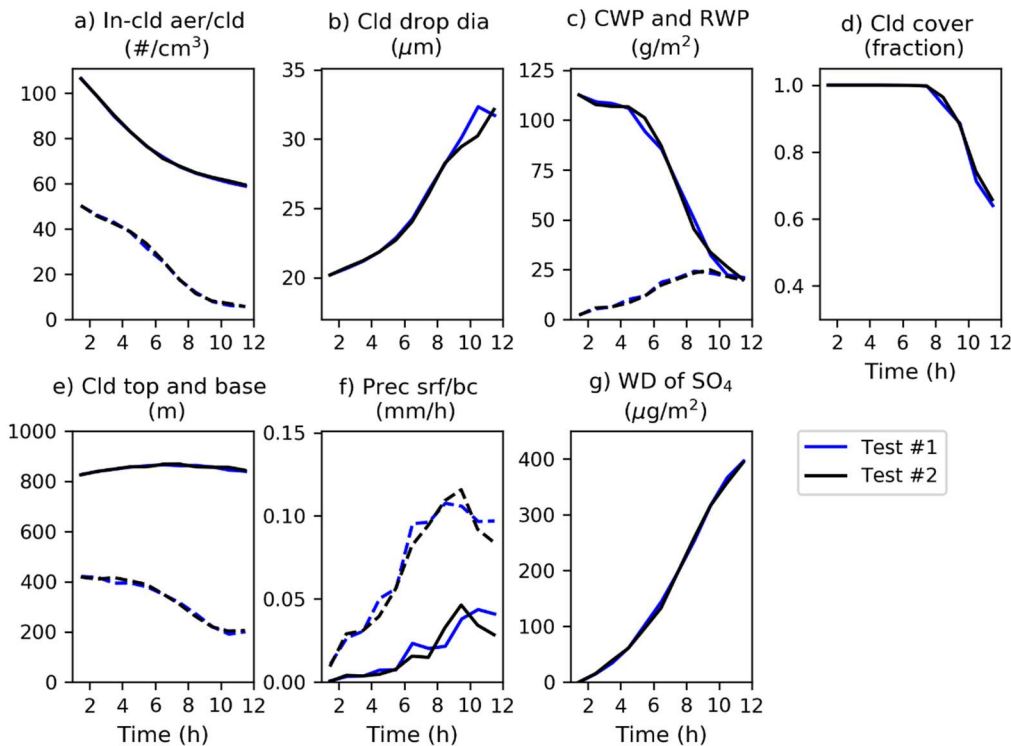


Figure S3. Timeseries of two simulations that differ only by the random perturbations used to initialize the turbulence.

S1.3 Autoconversion parameterization

While the bin scheme in UCLALES-SALSA describes accurately particle dry-size distribution, in the presented simulations we applied the autoconversion parameterization of Seifert and Beheng (2001) that is based on total droplet number and mass and thus does not resolve their size spectrum. Thus, it is not optimal for modelling the effect of the giant cloud condensation nuclei (GCCN). However, UCLALES-SALSA includes an alternative, more mechanistic option for simulating droplet growth from cloud droplet to small drizzling droplet. This scheme has been used previously for studying cloud seeding (Tonttila et al., 2021) and in a aerosol-cloud closure study by (Calderón et al., 2022). It is based on explicitly counting all collisions between cloud droplets where the product is large enough (>20 microns in wet diameter) to start efficiently collecting other droplets to form drizzle and rain. This collision rate limited scheme requires much longer spin-up to build up realistic cloud and drizzle droplet size distributions than employing the autoconversion parameterization that grows a subpopulation of cloud droplets instantly to wet sizes above 50 micrometers.

As the current study required a large number of simulations and GCCN effects were relevant for only small fraction of those, we used the Seifert-Beheng parameterization to reduce computational burden. However, as the GCCN effect seemed to play a

small but noticeable role in creating the difference between the no-emission control case and the simulation with Gong (2003) sea spray emission, we repeated these simulations together with the base case with Fuentes et al. (2010) sea spray emission using the more mechanistic scheme. Figure S4 and Figure S5 show the simulations using the Seifert-Beheng parameterization and the collision-based scheme respectively. Figure S4 indeed shows relatively minuscule effects of the GCCN.

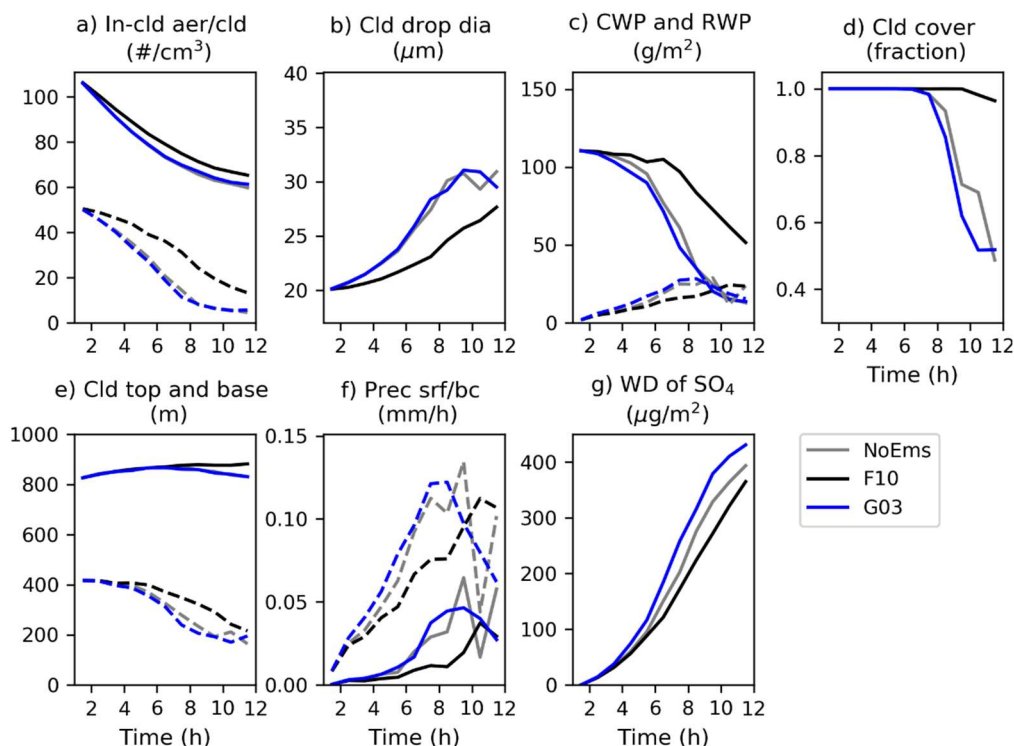


Figure S4. Simulations with the Seifert-Beheng autoconversion parameterization. Hourly averaged time series, mean over the model area. Panels: a – in-cloud cloud interstitial aerosol (solid) and cloud droplet (dashed) concentration, b – Cloud droplet size, c – Cloud liquid water path (solid) and rain water path (dashed), d – height of cloud top (solid) and base (dashed), e – precipitation rate at surface (solid) and below cloud (dashed), f – cumulative wet deposition of background aerosol (ammonium bisulfate). Simulations: grey – no-emission control, black – F10, Blue – G03 setups. All schemes were run with SST 10°C and 10 m/s windspeed.

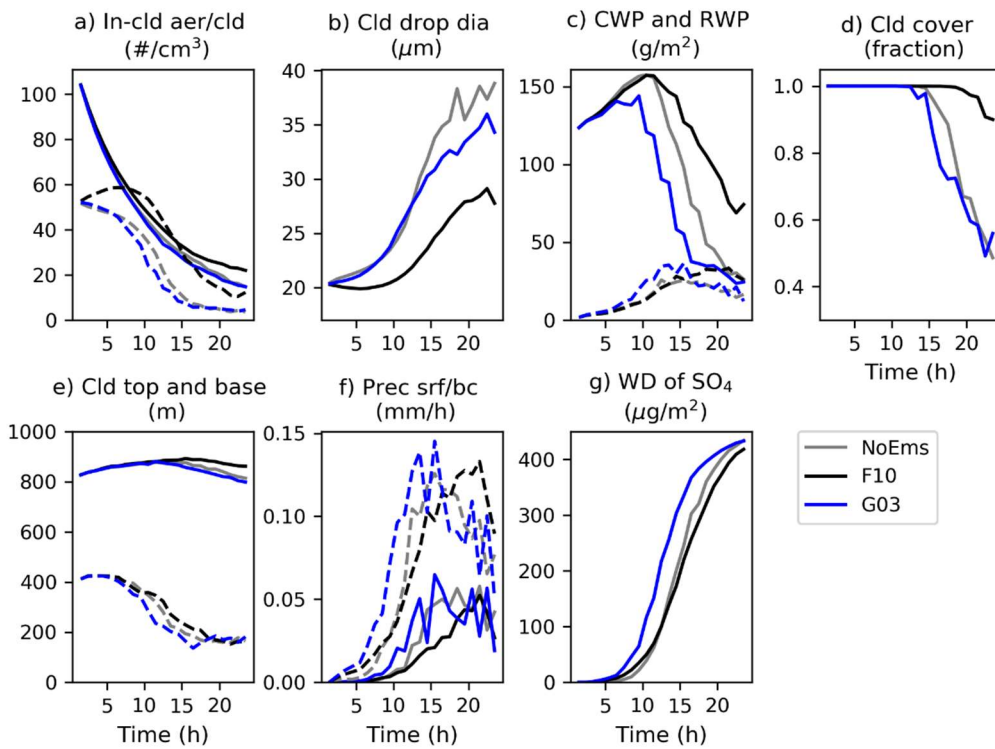


Figure S5. Simulations using explicit precipitation formation scheme. Panels and line colours are the same as in Figure S4

As seen from Figure S5, with the mechanistic scheme it takes about twice longer in the no-emission case (gray line) before the clouds start restructuring and significant levels of precipitation occur. And in this case the effect of the GCCN emitted by the Gong (2003) sea spray scheme (blue line) is indeed much more noticeable, speeding up the appearance of surface precipitation by several hours. An indication of GCCN effect is also visible for the F10 case (black) where low levels of below-cloud drizzle are visible hours before the precipitation occurs in the no-emission case. In this case the GCCN effect competes with the rain-delaying effects of the extra CCN from fine sea spray and thus stronger surface-reaching drizzle still starts a couple of hours later than it occurs in the no-emission control, similarly to the main simulations.

The large difference in the mean cloud droplet size when using the different schemes is due to using different definitions for drizzle – in the case of the Seifert-Beheng scheme the raindrop size spectrum starts from 50 microns wet diameter and all droplets produced by the autoconversion scheme are assumed to be this size. In the simulations with the mechanistic scheme the drizzle bins are used for coalescence-growth dominated size-range and start from 20 microns wet diameter. All droplets that reach this size by collision-coalescence process are moved from cloud bins to drizzle bins, while purely condensational growth is still handled in the cloud bins, as condensation affects the whole population in the bin uniformly and the wet-size distribution does not widen. This classification is not expected to be a source of error as all microphysical processes are

computed identically for both cloud droplets and drizzle and only the bin limits are defined differently based on dry size (cloud droplets) or wet size (drizzle/precipitation).

S2. Gas phase chemistry

Table S1. VOC oxidation reactions and stoichiometric coefficients. Reaction rate k ($\text{cm}^3 \text{molec}^{-1} \text{s}^{-1}$) at temperature T is obtained as follows: $k(T) = k_{298} * \exp(E/T)$.

Reaction		Rate		Stoichiometric coefficients				
		k_{298}	E	VBS0	VBS1	VBS10	IEPOX	Glyoxal
Isoprene	OH	$2.7^{\text{a)}$ $\times 10^{-11}$	390	$^{\text{b)}$	$^{\text{b)}$	$^{\text{b)}$	$0.525^{\text{e)}$	$0.025^{\text{h)}$
Isoprene	O ₃	$1.03^{\text{a)}$ $\times 10^{-14}$	-1995	0.0	0.0295	0.0453	-	-
Isoprene	NO ₃	$3.15^{\text{a)}$ $\times 10^{-12}$	-450				-	-
Mono- terpenes	OH	$1.2^{\text{a)}$ $\times 10^{-11}$	440	$^{\text{c)}$	$^{\text{c)}$	$^{\text{c)}$	-	-
Mono- terpenes	O ₃	$6.3^{\text{a)}$ $\times 10^{-16}$	-580	0.1	0.037	0.088	-	-
Mono- terpenes	NO ₃	$1.2^{\text{a)}$ $\times 10^{-12}$	490				-	-
IEPOX	OH	$1.25^{\text{d)}$ $\times 10^{-11}$	-	-	-	-	-	$0.24^{\text{g)}$
Glyoxal	OH	$3.1^{\text{f)}$ $\times 10^{-12}$	340	-	-	-	-	-
Glyoxal	NO ₃	$4.0^{\text{f)}$ $\times 10^{-16}$		-	-	-	-	-

a) Atkinson et al. (2006)

b) Interpolated from Henze and Seinfeld (2006)

c) Kokkola et al. (2014)

d) Bates et al. (2014), average of cis and trans isomers

e) Paulot et al. (2009)

f) IUPAC (2022)

g) Jacobs et al. (2013)

h) Jenkin et al. (2015)

S3. References

- Ackerman, A. S., van Zanten, M. C., Stevens, B., Savic-Jovicic, V., Bretherton, C. S., Chlond, A., Golaz, J. C., Jiang, H., Khairoutdinov, M., Krueger, S. K., Lewellen, D. C., Lock, A., Moeng, C. H., Nakamura, K., Petters, M. D., Snider, J. R., Weinbrecht, S. and Zulauf, M.: Large-eddy simulations of a drizzling, stratocumulus-topped marine boundary layer, *Mon. Weather Rev.*, 137(3), 1083–1110, doi:10.1175/2008MWR2582.1, 2009.
- Atkinson, R., Baulch, D. L., Cox, R. A., Crowley, J. N., Hampson, R. F., Hynes, R. G., Jenkin, M. E., Rossi, M. J., Troe, J. and Subcommittee, I.: Evaluated kinetic and photochemical data for atmospheric chemistry: Volume II – gas phase reactions of organic species, *Atmos. Chem. Phys.*, 6, 3625–4055, doi:10.5194/acp-6-3625-2006, 2006.
- Bates, K. H., Crounse, J. D., St. Clair, J. M., Bennett, N. B., Nguyen, T. B., Seinfeld, J. H., Stoltz, B. M. and Wennberg, P. O.: Gas phase production and loss of isoprene epoxydiols, *J. Phys. Chem. A*, 118(7), 1237–1246, doi:10.1021/jp4107958, 2014.
- Calderón, S. M., Tonttila, J., Buchholz, A., Joutsensaari, J., Komppula, M., Leskinen, A., Hao, L., Moiseev, D., Pullinen, I., Tiitta, P., Xu, J., Virtanen, A., Kokkola, H. and Romakkaniemi, S.: Aerosol-stratocumulus interactions : Towards a better process understanding using closures between observations and large eddy simulations, *Atmos. Chem. Phys. Discuss.* [preprint], in review, doi:https://doi.org/10.5194/acp-2022-273, 2022.
- Fuentes, E., Coe, H., Green, D., De Leeuw, G. and McFiggans, G.: On the impacts of phytoplankton-derived organic matter on the properties of the primary marine aerosol - Part 1: Source fluxes, *Atmos. Chem. Phys.*, 10(19), 9295–9317, doi:10.5194/acp-10-9295-2010, 2010.
- Gong, S. L.: A parameterization of sea-salt aerosol source function for sub- and super-micron particles, *Global Biogeochem. Cycles*, 17(4), 1–7, doi:10.1029/2003gb002079, 2003.
- Henze, D. K. and Seinfeld, J. H.: Global secondary organic aerosol from isoprene oxidation, *Geophys. Res. Lett.*, 33(9), 6–9, doi:10.1029/2006GL025976, 2006.
- IUPAC: Task group on atmospheric chemical kinetic data evaluation. (Ammann, M., Atkinson, R., Cox, R.A., Crowley, J.N., Herrmann, H., Jenkin, M.E., Mellouki, W., Rossi, M. J., Troe, J. and Wallington, T. J.), last accessed 15.07.2022, [online] Available from: <http://iupac.pole-ether.fr>, 2022.
- Jacobs, M. I., Darer, A. I. and Elrod, M. J.: Rate constants and products of the OH reaction with isoprene-derived epoxides, *Environ. Sci. Technol.*, 47(22), 12868–12876, doi:10.1021/es403340g, 2013.
- Jenkin, M. E., Young, J. C. and Rickard, A. R.: The MCM v3.3.1 degradation scheme for isoprene, *Atmos. Chem. Phys.*, 15(20), 11433–11459, doi:10.5194/acp-15-11433-2015, 2015.
- Kokkola, H., Yli-Pirila, P., Vesterinen, M., Korhonen, H., Keskinen, H., Romakkaniemi, S., Hao, L., Kortelainen, A., Joutsensaari, J., Worsnop, D. R., Virtanen, A. and Lehtinen, K. E. J.: The role of low volatile organics on secondary organic aerosol formation, *Atmos. Chem. Phys.*, 14(3), 1689–1700, doi:10.5194/acp-14-1689-2014, 2014.
- Paulot, F., Crounse, J. D., Kjaergaard, H. G., Kürten, A., Clair, J. M. S., Seinfeld, J. H. and Wennberg, P. O.: Unexpected epoxide formation in the gas-phase photooxidation of isoprene, *Science* (80-.), 325(5941), 730–733,

doi:10.1126/science.1172910, 2009.

Seifert, A. and Beheng, K. D.: A double-moment parameterization for simulating autoconversion, accretion and selfcollection, *Atmos. Res.*, 59–60, 265–281, doi:10.1016/S0169-8095(01)00126-0, 2001.

Stevens, B., Moeng, C. H., Ackerman, A. S., Bretherton, C. S., Chlond, A., de Roode, S., Edwards, J., Golaz, J. C., Jiang, H., Khairoutdinov, M., Kirkpatrick, M. P., Lewellen, D. C., Lock, A., Müller, F., Stevens, D. E., Whelan, E. and Zhu, P.: Evaluation of large-eddy simulations via observations of nocturnal marine stratocumulus, *Mon. Weather Rev.*, 133(6), 1443–1462, doi:10.1175/MWR2930.1, 2005.

Tonttila, J., Afzalifar, A., Kokkola, H., Raatikainen, T., Korhonen, H. and Romakkaniemi, S.: Precipitation enhancement in stratocumulus clouds through airborne seeding: Sensitivity analysis by UCLALES-SALSA, *Atmos. Chem. Phys.*, 21(2), 1035–1048, doi:10.5194/acp-21-1035-2021, 2021.